

## CURRENT EUROPEAN ROTORCRAFT RESEARCH ACTIVITIES ON DEVELOPMENT OF ADVANCED CFD METHODS FOR THE DESIGN OF ROTOR BLADES (BRITE/EURAM 'D A C R O' PROJECT)

Contributing Companies/Establishments:

MBB	NLR	Univ. of the Bundeswehr Munich
Agusta	ONERA	Univ. of Rome
CIRA	TRITECH	Westland
DLR	Univ. Of Bristol	Aerospatiale

Presented by G. Polz (MBB)

### Abstract

The work performed up to now in the BRITE/EURAM Pilot Phase project DACRO is described.

The activities focus on the development and validation of new computational fluid dynamics (CFD) codes for application to the aerodynamic environment of helicopter rotor blades. Additional tasks are the reviewing of the current computational methods, the definition of possible improvements, and the selection of appropriate data bases for code validation.

The theories applied by the partners are

- transonic small perturbation (TSP) theory
- unsteady full potential theory
- Euler methods

Based on these theories, the development of new codes and the improvement of existing codes has been undertaken by the partners.

In this paper primarily the methods in use are described and the progress achieved up to now is demonstrated.

### 1. Introduction

A twelve-partner-programme for CFD applications on rotorcraft blades was started in 1990 in the BRITE/EURAM Pilot Phase under the name DACRO (Development of Advanced CFD Methods for the Design of Rotorcraft Blades).

Presented at the 17th European Rotorcraft Forum, 24 - 27 September 1991, Berlin, Germany

The work began with a review of the existing methods for the flow around helicopter rotor blades, followed by establishing the requirements of the capabilities of improved and newly developed codes. The existing and available experimental data were reviewed and appropriate common test cases from hover and forward flight were selected for the validation of the codes.

The main aim of these studies is a better understanding of the physics in the flow around helicopter rotor blades. Fig. 1 shows the main objectives as defined for the DACRO programme.

---

#### DEVELOP OR IMPROVE ADVANCED CFD METHODS FOR:

- a better understanding and prediction of the three-dimensional, unsteady, transonic, viscous blade flow phenomena
- an availability of design tools for advanced rotor blade airfoils and tip shapes

⇒ ROTOR PERFORMANCE IMPROVEMENTS, VIBRATORY LOADS AND NOISE REDUCTIONS

---

Fig. 1 Main objectives of the DACRO research programme

For the cooperation in the DACRO programme, three different tasks were defined (Fig. 2), and three groups of partners were established for the collaborative work in each of the tasks.

Computational Methods and experimental data bases are considered for the following flow types and operational conditions:

- 2D flow conditions (steady and unsteady)
- 3D Hover conditions for non-lifting and lifting rotors
- 3D Forward flight conditions for non-lifting and lifting rotors

Fig. 2 Main tasks for the DACRO research programme

### 2. Targets for improvement and further development of computational methods

Global targets for the improvement of existing and the development of new CFD methods for rotor aerodynamics were defined at the beginning of the DACRO activities:

- adjustment of the codes to specific rotor flow conditions
- improvement of geometry discretisation
- extension of codes to higher level of complexity
- \* 2D --> 3D
- \* steady --> unsteady
- \* subsonic --> transonic
- \* non-lifting --> lifting
- \* inviscid --> viscid
- \* explicit --> implicit

A common definition was made for the results to be produced by the different methods used by the partners. Data of particular interest for comparison and validation of the codes are:

- Mach number distribution
- velocity vectors
- shock location
- pressure distribution (static and total pressure)
- boundary layer parameters
- wake geometry

All flow field quantities are required on the rotor blade surface as well as in the flowfield.

### 3. Experimental data bases selected for code validation

The test data bases selected as a common basis for the validation of the theoretical methods are shown in Fig. 3.

Experimental data for the 2D case were taken from unsteady measurements on NACA0012 and NACA64A010 airfoils (Ref. 1).

For the hover flight conditions data from NASA (Ref. 2) and from ONERA tests (Ref. 4) are selected. The NASA test data are acquired with a two-bladed untwisted model rotor with NACA0012 blade airfoil.

FLOW CONDITION	EXPERIMENTAL DATA USED
2D steady and unsteady	steady and oscillating airfoil data (AGARD data bases)
3D hover for nonlifting and lifting rotors	<ul style="list-style-type: none"> <li>- US Army model rotor</li> <li>- ONERA model rotor with rectangular and non-rectangular blades</li> </ul>
3D forward flight for non-lifting and lifting rotors	non-lifting and lifting results for ONERA model rotor with rectangular and non-rectangular blades

Fig. 3 Experiments selected for code validation in the DACRO programme

For the non-lifting forward flight configurations, experimental results available at ONERA (Ref. 3) are used for the validation of the computer codes. The selected test cases concern a two-bladed rotor in high speed forward flight. Two blade shapes were considered: a tapered one without any sweep and a set of blades with a 30 deg sweptback tip (Fig. 4). These blades are untwisted with NACA00XX airfoils and equipped with absolute pressure transducers at the spanwise stations .85 R, .90 R, and .95 R.

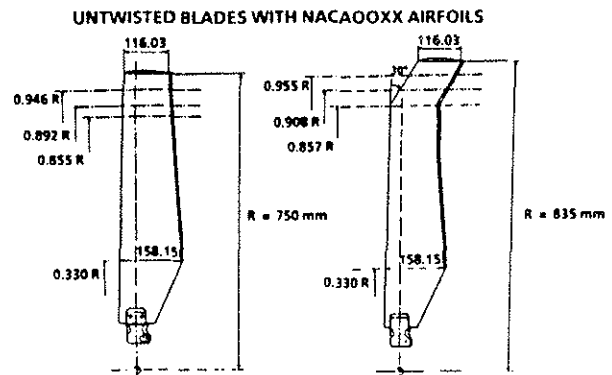


Fig. 4 Blade geometry of two-bladed ONERA model rotors (Ref. 3)

At high forward flight speed, the power needed to drive the rotor is higher with the straight blades than with the 30 deg sweptback tip ones. This is due to the difference of the unsteady transonic wave intensity on the advancing blade side with the two different tip shapes (Fig. 5). On the sweptback tip, the transonic wave intensity is decreased on a large part of the advancing blade side and is shifted towards the second quadrant (azimuth > 90 deg).

The test cases selected for the codes validation correspond to advance ratios of .4, .45, and .5. Measured unsteady pressure distributions on the two different blades are available for comparison with the theoretical ones.

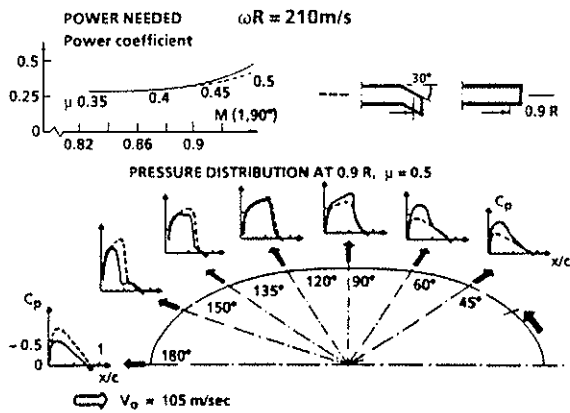


Fig. 5 Measured pressure distribution and power consumption in forward flight for two-bladed ONERA model rotors

For the lifting hover and forward flight configurations, experimental results available at ONERA (Ref. 4) for a rectangular and a parabolic sweptback tip with anhedral effect were considered. The planform shape of the parabolic tip is defined in Fig. 6. The leading edge sweep is about 80 deg at the tip and the chord is half the one of the main part of the blade. Pressure measurements performed at spanwise stations .85 R, .90 R, and .95 R are available to validate the different codes for lifting configurations.

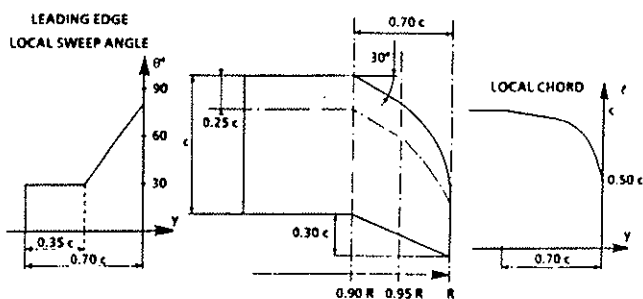


Fig. 6 Geometry of three-bladed ONERA model rotor PF1 blade tip (Ref. 4)

#### 4. Two-dimensional flow conditions

Two-dimensional steady and unsteady investigations are carried out to determine the feasibility of various mathematical and physical models to predict transonic and viscous effects on rotor loads (Fig. 7).

#### Computational Methods:

- Boundary element method including transonic effects
- Unsteady small perturbation theory with and without boundary layer
- Unsteady Euler code

#### Data bases:

- Steady and oscillating airfoil data (AGARD data bases)

Fig. 7 Computational methods and experimental data bases applied for 2D flow conditions

As a typical result of the validation of various two-dimensional flow computer codes, Fig. 8 shows the time history of unsteady lift and moment coefficients for the NACA0012 airfoil oscillating in pitch at transonic conditions. The experimental data (Ref. 1) indicate flow separation near the maximum angle of attack.

#### Unsteady transonic small perturbation method

Computations were carried out using a computer code based on the unsteady transonic small perturbation (TSP) theory, coupled in strong interaction with an integral method for the unsteady turbulent boundary layer (Ref. 5). The inviscid results exhibit large differences compared with the experimental data (Fig. 8). The differences are mainly due to the prediction of too strong shock waves located too far downstream, and when neglecting viscous effects. By including the effects of a boundary layer in the TSP method, the unsteady lift is well predicted including the light stall behaviour near the maximum angle of attack. The moment coefficient is somewhat less well predicted.

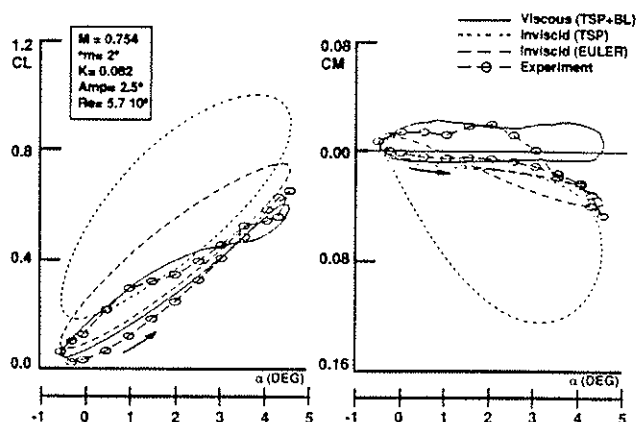


Fig. 8 Unsteady airloads on oscillating NACA0012 airfoil

### Unsteady Euler code

In order to develop a 2D unsteady algorithm for the calculation of the flow past an oscillating airfoil, the Euler equations are transformed into a moving blade attached coordinate system such that the vector of dependent variables does not contain rotational velocities (Ref. 8). The approximations of the spatial and the time dependent terms are decoupled. Dissipative terms are explicitly introduced to avoid spurious oscillations. For the formulation of the unsteady code an existing 2D steady Euler code was extended to time accurate calculations. In order to allow larger global time steps, an implicit residual damping with variable coefficients, which are chosen time and grid dependent, has been integrated.

Several test cases have been calculated for the validation of the code. The results exhibit some differences compared with the experimental data (Fig. 8), but they agree relatively better with the experiment than the TSP results. The differences can primarily be referred to disregarding the viscous effects.

### 5. Three-dimensional hover conditions of non-lifting and lifting rotors

The theoretical methods, investigated for modelling of the 3D steady flow on lifting and non-lifting rotors, and the corresponding experiments are listed in Fig. 9.

#### Computational Methods:

- Boundary element method
- Transonic small perturbation theory coupled with a global rotor code for lifting cases
- Full potential theory
- Explicit/Implicit Euler codes

#### Data bases:

- US Army model rotor
- ONERA model rotor with rectangular and non-rectangular blades

Fig. 9 Computational methods and experimental data bases applied for 3D hover flight conditions

### Potential flow solutions with boundary element method

An algorithm for the aerodynamic analysis of an isolated rotor in hover using a boundary element methodology (BEM) is under development (Ref. 9). The flow is assumed to be potential, but compressible and transonic. The method solves the integral form of the wave equation for the velocity potential and a transonic small perturbation hypothesis is assumed in the treatment of the non-linear terms. The non-linear terms

result in volume integrals that require a boundary-element spatial discretization of the flow field surrounding the rotor blade (only in the blade tip region where the non-linear terms are important). The method has been applied up to now to steady transonic 2D airfoil cases with encouraging results.

### Transonic small perturbation method

The mathematical model solves the transonic small perturbation (TSP) approximation to the potential flow equation for the flow over a helicopter rotor blade in hover and forward flight (Ref. 6). An ordering scheme has been applied to simplify the final equation to be solved.

A typical result from the NASA hover non-lifting test cases (Ref. 2) is shown in Fig. 10 (top). In general, excellent correlation between the TSP and test data was observed for all cases examined.

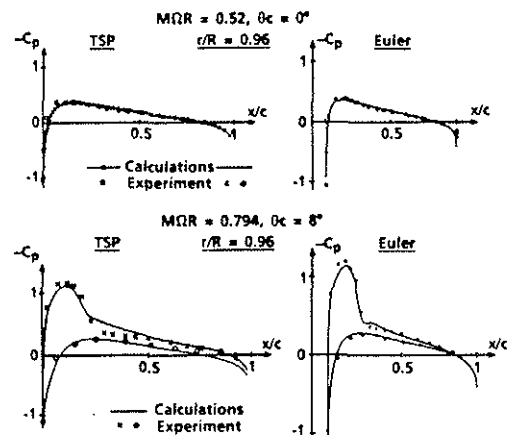


Fig. 10 Comparisons of calculated pressure distributions with experimental results for non-lifting (top) and lifting (bottom) two-bladed rotor

In order to carry out lifting calculations, the influence of the complex wake system has to be taken into account. Since the TSP code implicitly includes the near wake effects, only the influences due to the intermediate and far wake have to be evaluated. The TSP code incorporates the wake effects by means of an effective angle-of-attack approach. In this code, the effective incidence is prescribed for different spanwise locations by an external wake loads code, which is based on a prescribed wake model. The wake effect is calculated by matching the experimental thrust coefficient with that calculated by the wake loads code. A typical result from the lifting calculations and its comparison with results from NASA test data (Ref. 2) is presented in Fig. 10 (bottom). In fact, the results show very good agreement everywhere around the shock region. This

is somewhat unexpected if one considers the relatively simple way with which the intermediate and far wake effects were accounted for in the TSP calculation.

### Three-dimensional Euler codes

Three different Euler codes are under development for the aerodynamic conditions of non-lifting and lifting rotors in hover flight

For the first code, the governing equations are the unsteady Euler equations in integral conservation form, referred to a blade-attached Cartesian frame, which is rotating with a constant angular velocity (Ref. 7). The equations are formulated such that the vector of dependent variables does not contain the rotational velocity. In order to damp out high frequency oscillations in the flow variables and to avoid oscillations in the neighbourhood of shock waves, dissipative terms are added. In the blade-attached coordinate system with constant angular velocity, the flow field of a hovering rotor is steady. Various techniques, like local time-stepping, implicit residual averaging and rothalpy damping are used to accelerate the convergence to steady state.

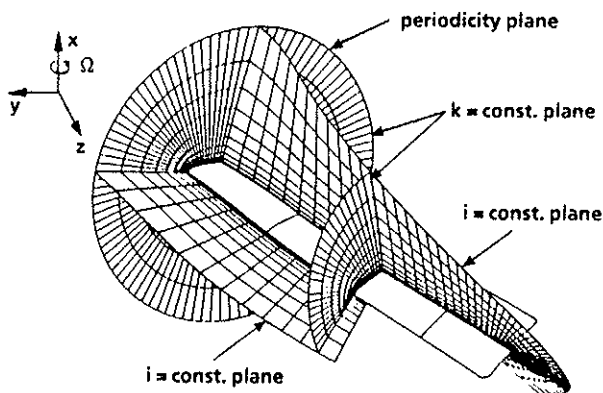


Fig. 11 Selected coordinate planes of an O-grid around a twisted blade

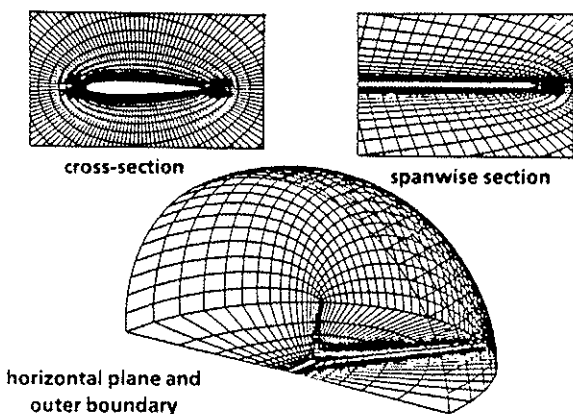


Fig. 12 O-grid arrangement for a two-bladed rotor in hover flight

The code has been applied to the two-bladed NASA model rotor. The grid for this calculations was generated with an algebraic grid generator which uses an O-O grid topology and is suited to two-bladed rotors or propellers only. Fig. 11 shows selected coordinate planes of a grid around a twisted blade. The O-structure of the grid in cross section and around the tip is obvious. A view of a cross section, a spanwise section, the horizontal and the farfield boundary is given in Fig. 12.

Calculations have been performed on a 128x32x36 cell grid for non-lifting and lifting conditions.

Fig. 13 shows the comparison of calculated and measured surface pressure distributions for the non-lifting case at three different radial stations. The agreement between the inviscid calculations and the experiment is excellent, since due to the low pressure gradients the influence of viscosity is small.

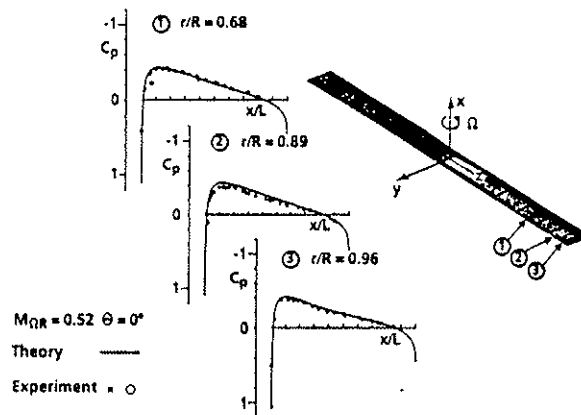


Fig. 13 Comparison of Euler calculation with experimental results on non-lifting rotor

Figure 14 shows the comparison between theory and measurement for a lifting case. Also chord-wise pressure distributions at three different radial stations are plotted. For this operational conditions the flow is transonic in the blade tip region. Experimental data and numerical results are in good agreement. The location and strength of the shock wave is predicted reasonably well with the present inviscid method. A flexible grid generation package for two-bladed and three-bladed rotors has been developed. An H-O grid topology has been selected, with O-type in cross sections and H-type in spanwise direction. Algebraic techniques are used to generate a starting mesh for the elliptic grid generation procedure (Ref. 10). This package has been used to generate a grid for the three-bladed ONERA rotor. Computations on this grid are going to be performed.

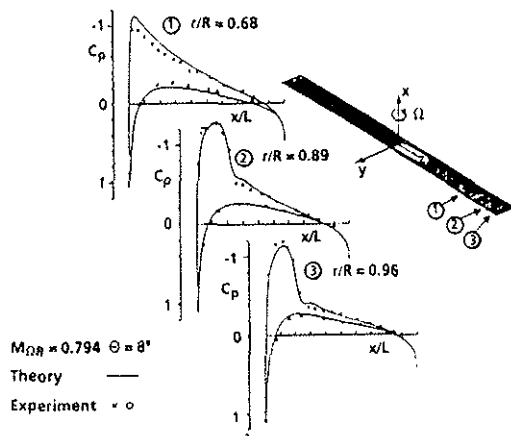


Fig. 14 Comparison of Euler calculation with experimental results for lifting in hover flight

The second code solves a three-dimensional pseudo-unsteady system for the compressible Euler equations formulated in a rotating frame and including only the mass and momentum equations. In this pseudo-unsteady system, only consistent with a steady-state solution for rotor in hover, the energy equation is replaced by the Bernoulli relation which states that the total rothalpy is constant all over the flow.

The numerical method, applied on a structured grid in the finite-volume approach, is based on a space-centered implicit scheme of second order accuracy, previously developed for steady transonic flows around airfoils (Ref. 11) and wings (Ref. 12). This original method can approximate steady weak solutions without artificial viscosity, since its internal dissipation is sufficient when the CFL number is large enough. Moreover, the implicit scheme allows great efficiency in computing steady solutions.

For application of the Euler code to the case of a multi-bladed rotor in hover, with pure capturing of vortex sheets and wake, the computational domain is restricted to the calculation of one blade only; the influence of other blades being taken into account through a periodic boundary condition.

In the third code (Ref. 13), the Euler equations are used in the differential conservation form. In order to have a hyperbolic system everywhere throughout the flowfield, the unsteady formulations of the Euler equations are chosen, even if only the steady solution is to be obtained. The solution algorithm is a finite volume method with the flow quantities referring to the cells center. Due to the character of rotating flow, a blade-attached cylindrical coordinate system, rotating with constant angular velocity  $\omega$  is chosen. Because of symmetry effects, the use of only one cylinder half is

sufficient, when considering a two-bladed rotor in hover. This requires a periodical boundary condition for the flow values at the plane of symmetry.

The code was tested both on non-lifting and lifting cases of hovering rotors. As the NASA model rotor is fitted with symmetric blade airfoil without twist, no tip vortex or blade-vortex interaction occurs in the non-lifting case. This case is suitable for testing numerical insufficiencies like accumulating errors, problems with numerical stability or influences of the far field. A good agreement of the computed results with the measured ones was achieved, demonstrating the accuracy of the applied Euler code.

The capability of the method to predict shocks, wake effects, and blade-vortex interactions was tested on a lifting rotor test case. Shock position and strength are well reproduced due to the used upwind scheme. Wake effects and blade-vortex interactions are included in the code without any additional external model. Recent results showed, that the pressure minimum is generally underpredicted in the outer blade sections. To improve the accuracy of the method, the influences of the local mesh refinement of the far-field, the extension of the grid, the tip shape or the numerical dissipation of the tip vortex are presently being investigated.

#### 6. Three-dimensional forward flight conditions of non-lifting and lifting rotors

Studies on the 3D unsteady airloads of non-lifting and lifting rotors in forward flight are conducted with the theoretical methods and data bases listed in Fig. 15.

##### Computational Methods:

- Quasi-steady and unsteady transonic small perturbation theory
- Unsteady full potential theory with and without boundary layer effects
- Unsteady Euler codes

##### Data bases:

- Non-lifting and lifting results for ONERA model rotor with rectangular and swept back blade tip shapes

Fig. 15 Computational methods and experimental data bases applied for 3D forward flight conditions

#### Transonic small perturbation method

The mathematical model solves the transonic small perturbation (TSP) approximation to the potential flow equation for the flow over a helicopter rotor blade at arbitrary azimuth in hover and forward flight. An ordering scheme has been applied to simplify the final equation to be solved. The basic equation includes the spanwise flow terms, which are essential to the model

ling of blade azimuth away from the advancing blade, but excludes any time dependent terms. A more detailed description of the method is given in Ref. 6.

Using the TSP code, the ONERA forward flight non-lifting test cases were evaluated for the rectangular and swept-back blades. Selected results of the chordwise pressured distribution are given shown in Fig. 16. It is found that the code gives good results over the flow regions where unsteady flow effects are small, i.e. in the first quadrant of the disk. It was also observed that the code predicted reasonably well the strength of any shocks present, but not their chordwise location. Since this TSP formulation is cast in a non-conservative form, this is not entirely unexpected.

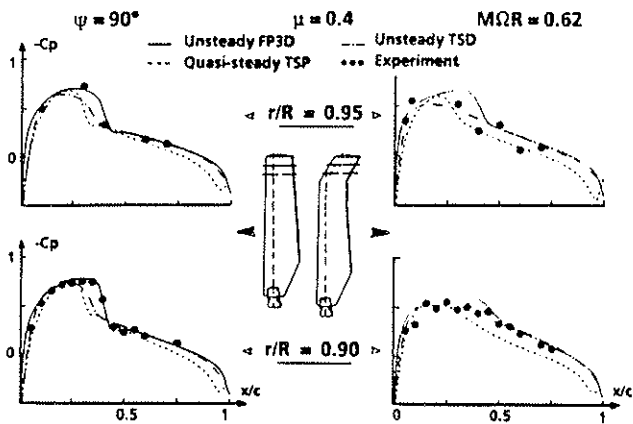


Fig. 16 Calculated Mach number distribution around rectangular blade tip in non-lifting forward flight

#### Unsteady full potential theory

The FP3D code solves the three-dimensional unsteady full potential equation (Ref. 14 and 15). The potential formulation assumes that the flow is isentropic and irrotational, a hypothesis generally valid for the advancing side of a helicopter rotor blade, as far as the local Mach number is less than 1.3. The equation is written in a generalized coordinate system in fully implicit and conservative form. It is discretized with second order accuracy in space and first order in time finite differences. A monotone Enquist-Osher flux biasing scheme is applied in supersonic regions to represent the domain of dependency correctly. The system is approximately factored into three one-dimensional operators so that its inversion is easier. At the grid boundaries, non-reflecting boundary conditions are applied to allow disturbance waves to get out of the computational domain. The computation is made on an isolated blade and therefore, for lifting cases, an external wake model is necessary to represent the inflow on the blade.

Figure 17 shows the Mach number distribution on and around the advancing rectangular blade for the three azimuth positions at an advance ratio of  $\mu = 0.5$ . The domain plotted extends from  $0.5 R$  to  $1.5 R$  on cylinders centered at the rotor hub. At the azimuth  $\psi = 60$  deg, the supersonic zone is developing on the blade, and the shock wave, not yet well established, is moving toward the blade trailing edge. At  $\psi = 90$  deg and  $120$  deg, a strong shock wave can be seen which, after  $90$  deg, is moving back toward the leading edge. Furthermore, the supersonic pocket on the blade is then connected to the supersonic zone off the blade, allowing thus acoustic waves to propagate into the farfield.

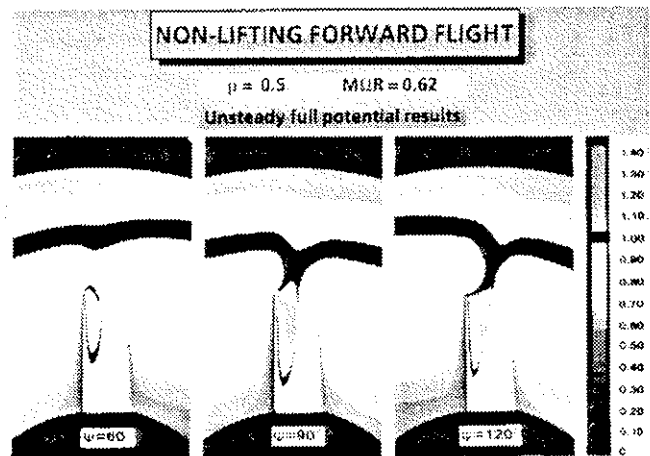


Fig. 17 Chordwise pressure distribution on advancing blade of non-lifting rotor, comparison of several theoretical results with experiments

Figure 16 shows some comparisons between experimental and theoretical results for the two blade planforms at  $90$  deg azimuth position. The pressure distributions obtained with an unsteady full potential code (FP3D), an unsteady transonic small disturbances code (TSD), and a quasi-steady small perturbation theory (TSP) are compared with the experimental results. The three codes predict the decrease of the transonic waves on the sweptback tip, with the full potential method giving slightly stronger shocks and better agreement with experiment.

The improvement of the results with the full potential code is confirmed in Fig. 18, where the pressure coefficients at different chord locations at the spanwise station  $.95 R$  are plotted versus azimuth. The shock motion (backwards before  $\psi = 90$  deg and forward after) and the non-symmetry between the 1st and 2nd quadrants are better predicted with the unsteady full potential code than with the small disturbances code.

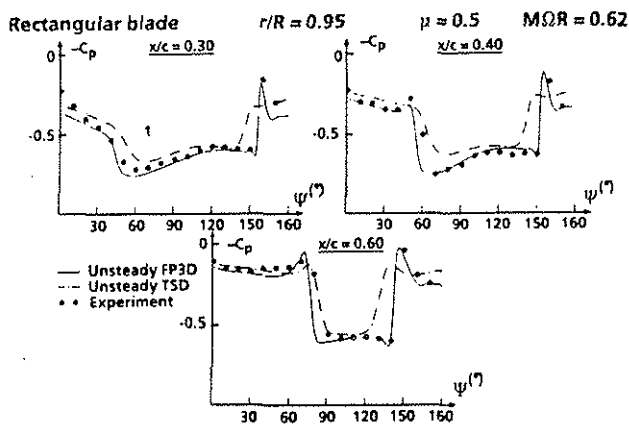


Fig. 18 Pressure at 30 % chord vs azimuth angle on rotor blade tip in non-lifting condition, comparison of full potential theory and experiment

### Unsteady Euler code

A 3D Euler code for the steady rotor flow (Ref. 16) was extended to unsteady flow conditions. The steady code was based on a 3D fixed wing code, and was tested against experimental results of model rotors in non-lifting and lifting hover flight with some success. Flux splitting is applied for reducing the complexity of the Euler equations. A finite volume method based on an Eigenvalue decomposition of the equations is used for solving the partial differential equations. The time integration is performed explicitly as a one-step scheme. The accuracy of the code is of first order in time and of second order in space. The cube-shaped 3D grid is generated analytically.

First computations with the code are performed for a two-bladed rotor with rectangular blade tip under non-lifting conditions with a tip Mach number in hover of  $M = 0.624$  and an advance ratio of  $\mu = 0.4$ .

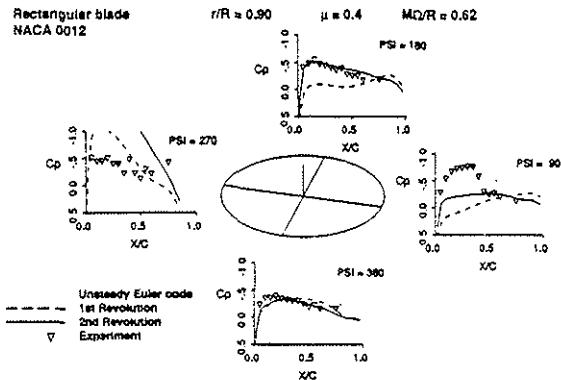


Fig. 19 Chordwise pressure distribution on rotor blade tip in non-lifting condition, comparison of unsteady Euler calculation with experiment

An H-type grid of 42x26x24 cells was used with a chordwise resolution of 18 points each on the upper and lower surface of the blade. Figure 19 shows the development of the pressure distribution during two revolutions starting from the initial guess. The computer run time required for the unsteady code is tremendous and thus hardly payable on a high performance computer. On a workstation computer the code is running more than 100 hours for one rotor revolution. The calculations are still going on and full convergence is expected after about six revolutions with the present grid fineness. The convergence trend seems to be faster at azimuth positions of 0 deg and 180 deg, whereas the solution builds up slower at the more critical flow conditions of the advancing and retreating blade.

Several measures to accelerate the calculation are being investigated, such as an implicit version of the code and different grid types.

### 7. Conclusions

The work performed up to now in the BRITE/EURAM project DACRO is described. The general progress achieved in this programme is the development of a range of CFD design tools for advanced helicopter rotor blade airfoils and tip shapes, with a better understanding and prediction of the complex flow phenomena. The DACRO activities should lead to a reduction in

- rotor power consumption, improving helicopter operational economy
- vibratory loads
- noise

This shall support for a better acceptance of the helicopter

In a continuation of the DACRO work, the present CFD methods shall be extended or new ones shall be developed for the prediction of aerodynamic and dynamic performance in hover and forward flight. These advanced methods shall be coupled with dynamic codes for the prediction of the aeroelastic behaviour of the rotor blades. Main problems to be addressed here are:

- dynamic stall
- rotor wake effects including blade vortex interactions
- unsteady viscous effects

- prediction of power required, loads and noise emission

For the BRITE/EURAM Intermediate Phase, a concrete programme for the continuation of the DACRO work is being developed presently at the institutions involved in helicopter aerodynamics.

## 8. References

1. AGARD, Compendium of unsteady aerodynamic measurements, AGARD R-702, data set 3 (1982)
2. Caradonna, F.X., Tung, C., Experimental and analytical studies of a helicopter rotor in hover, NASA TM-81232, 1981
3. Philippe, J.J., Chattot, J.J., Experimental and theoretical studies on helicopter blade tips at ONERA, 6th European Rotorcraft Forum, Bristol, September 1980
4. Desopper, A., Lafon, P., Philippe, J.J., Prieur, J., Effect of anhedral swept back tip on the performance of a helicopter rotor, 13th European Rotorcraft Forum, Arles, September 1987
5. Houwink, R., van Egmond, J.A., van Gelder, P.A., Computation of viscous aerodynamic characteristics of 2-D airfoils for helicopter applications, NLR MP 88052 U (1988)
6. Grant, J., The prediction of supercritical pressure distributions on blade tips of arbitrary shape over a range of advancing blade azimuth angles, *Vertica*, Vol. 3, pp 275 -292, 1979
7. Kroll, N., Berechnung von Strömungsfeldern um Propeller und Rotoren im Schwebeflug durch die Lösung der Euler-Gleichungen, DLR-FB 89-37 (1989)
8. Pahlke, K., Development of a numerical method solving the unsteady Euler equations for oscillating airfoils, DLR-IB 129-90/35 (1990)
9. Iemma, U., Un Metodo agli Elementi di Contorno per l'Analisi di Problemi Stazionari Transonici, Tesi di Laurea, Università di Roma La Sapienza, Dipartimento di Meccanica e Aeronautica (in Italian), May 1990
10. Pahlke, K., Grid generation for multi-bladed rotors and calculations with a 3-D Euler code for helicopter rotors in hover, DLR-IB 129-91/04 (1991)
11. Lerat, A., Sides, J., Efficient solution of the Euler equations with a centered implicit method, In: *Num.Meth.Fluid Dyn. III*, R.K.W. Morton and M.J. Baines (Eds), Clarenton Press, Oxford, pp.65-86, (Also TP ONERA 1988-128)
12. Lerat, J., Sides, J., Boniface, J.C., Transonic Euler solutions for ONERA M6 wing by an implicit space-centered method without artificial viscosity, *La Recherche Aérospatiale*, 1991 (in preparation)
13. Krämer, E., Theoretische Untersuchungen der stationären Rotorblatsumströmung mit Hilfe eines Eulerverfahrens, Dissertation, Universität der Bundeswehr München, Institut für Luftfahrttechnik, Neubiberg 1991
14. Costes, M., Jones, H.E., Computation of transonic potential flow on helicopter rotor blades, 13th European Rotorcraft Forum, Arles, September 1988
15. Costes, M., Desopper, A., Ceroni, P., Lafon, P., Flow field prediction for helicopter rotor with advanced tip shapes using CFD techniques, 2nd International Conference on Basic Rotorcraft Research, College Park (University of Maryland), February 1988
16. Stahl-Cucinelli, H., Application of 3D Euler code to rotor blade tips, 15th European Rotorcraft Forum, Amsterdam, September 1989

**Acknowledgement** - The DACRO partners wish to acknowledge support for this research work by the European Community.